Scheme I

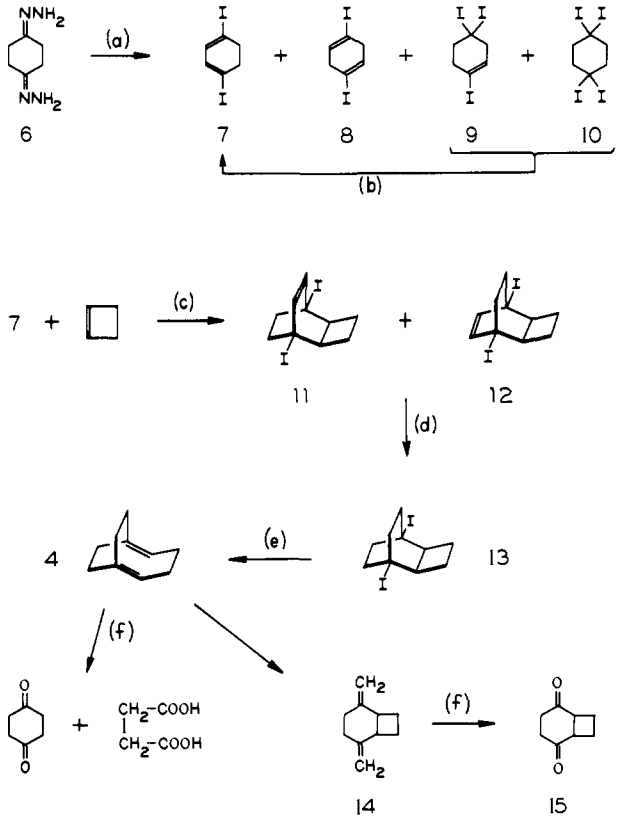

[a] (a) Iodine, triethylamine. (b) 1,5-Diazabicyclo[4.3.0]non-5-ene. (c) 100 °C, 30 days. (d) Diimide. (e) *tert*-Butyllithium, dimethyl ether, −78 °C. (f) Ozone.

°C gave cyclohexane-1,4-dione and succinic acid. No dione **15** was found. Diene **4** is thermally labile and very sensitive to oxygen and has not yet been isolated in a pure state. Attempts to purify **4** by gas chromatography caused isomerization to **14**: ^{1}H NMR δ 4.78 (4 H, br s), 3.06 (2 H, br s), 2.45-1.96 (8 H, complex). Ozonolysis of **14** gave dione **15.** The double bonds of **4** are held rigidly parallel and face to face facilitating the Cope rearrangement.

Partial purification of diene **4** after generation from **13** at −78 °C was accomplished by distillation at −25 °C. The vinyl protons of **4** resonate at δ 5.4 in the ^{1}H NMR spectrum. A Raman spectrum of a mixture of **4** and **14** shows bands at 1620 and 1637 cm^{-1}, which are assigned to the double-bond stretching frequencies of **4** and **14**, respectively. Warming the sample caused the band at 1620 cm^{-1} to decrease, while the band at 1637 cm^{-1} increased.

The rate of rearrangement of **4** into **14** has been measured by ^{1}H NMR spectroscopy by integrating the resonances for the vinyl hydrogens of **4** and **14** using benzene as an internal standard. The reaction rates are shown in Table I. The decrease in the resonance at δ 5.4 is accompanied by twofold increase in the resonance at δ 4.78 and, within the limits of the NMR method, the isomerization of **4** into **14** is quantitative.

In the deiodination of **13**, cleavage of either of the two ethano bridges of the bicyclo[2.2.2]octane ring system would lead directly to **14**. The exclusive formation of **4** by cleavage of the cyclobutano bridge of **13** is a remarkable example of kinetic product control in a reaction.

Table I. Reaction Rates for Isomerization of **4** into **14**

temp, °C	reaction rate, min^{-1}	$t_{1/2}$, min
25	2.2×10^{-3}	314
40	1.1×10^{-2}	64
E_a = 19.6 kcal/mol		

Acknowledgment is made to the donors of the Petroleum Research Fund, administered by the American Chemical Society, for partial support of this work, and to Badische Anilin Soda Fabrik AG for a gift of cyclooctatetraene used in the preparation of cyclobutene. J.J.V. thanks the University of Michigan for fellowships from the Frank Knoller and A. B. Prescott funds.

References and Notes

(1) J. Bredt, *Justus Liebigs Ann. Chem.*, **437**, 1 (1924).
(2) For reviews see (a) G. L. Buchanan, *Chem. Soc. Rev.*, **3**, 41 (1974); (b) G. Kobrich, *Angew. Chem., Int. Ed. Engl.*, **12**, 464 (1973); (c) J. Liebman and A. Greenberg, *Chem. Rev.*, **76**, 311 (1976).
(3) J. R. Wiseman and W. A. Pletcher, *J. Am. Chem. Soc.*, **92**, 956 (1970).
(4) Anita O. Sy, Ph.D. Dissertation, University of Michigan, 1977.
(5) R. L. Viavattene, F. D. Greene, L. D. Cheung, R. Majeste, and L. M. Trefonas, *J. Am. Chem. Soc.*, **96**, 4342 (1974).
(6) (a) F. Vögtle and P. Neumann, *Top. Curr. Chem.* **48**, 67 (1974); (b) B. H. Smith, "Bridged Aromatic Compounds", Academic Press, New York, 1964; (c) D. J. Cram and J. M. Cram, *Acc. Chem. Res.*, **4**, 204 (1971).
(7) (a) S. Masamune, D. W. Brooks, K. Morio, and R. L. Sobszak, *J. Am. Chem. Soc.*, **98**, 8277 (1976); (b) L. T. Scott and W. R. Brunsvold, *ibid.*, **100**, 4320 (1978).
(8) E. Vogel and H. D. Roth, *Angew. Chem., Int. Ed. Engl.*, **3**, 228 (1964).
(9) (a) G. M. Whitesides, G. L. Goe, and A. C. Cope, *J. Am. Chem. Soc.*, **91**, 2608 (1969); (b) N. L. Allinger and J. T. Sprague, *ibid.*, **94**, 5734 (1972).
(10) N. A. Domnin and N. S. Glebovskaya, *J. Gen. Chem. USSR (Engl. Trans.)*, **27**, 723 (1957).
(11) D. H. R. Barton, R. E. O'Brien, and S. Sternhell, *J. Chem. Soc.*, 470 (1962).
(12) All new compounds described had infrared, NMR, and mass spectra in accord with assigned structures, and, except for compounds **4** and **10**, elemental analyses within 0.3% of calculated values were obtained.

John R. Wiseman,* Jeffrey J. Vanderbilt
Department of Chemistry, University of Michigan
Ann Arbor, Michigan 48109
Received June 13, 1978

Isolation and Structure of Amoorastatin[1]

Sir:

An aqueous extract of *Aphanamixis grandifolia* Bl. seeds was found during an initial study to contain the novel cell growth (murine P388 lymphocytic leukemia) inhibitory tetranortriterpene aphanastatin (**1**).[2] Further investigation (directed by bioasay) of the same extract, from this interesting Eastern Himalayan (India) plant, for antineoplastic constituents has now led to discovery of a new limonoid[3] designated amoorastatin[4] (**2a**) with even greater cell growth (P388)[5] inhibitory (ED_{50} = <0.001 μg/mL) properties. We report that interpretation of spectral data and confirmation by single-crystal X-ray analysis has made possible an unequivocal assignment of structure **2a** (C-28 *R* and *S*) to amoorastatin: mp 205 °C (sintering from 170 °C, crystals from chloroform-methanol); CD in dioxane, Δ^ϵ −4.01 (300 nm) and −3.64 (310 nm).

High resolution mass spectrometry allowed assignment of molecular formula $C_{28}H_{36}O_9$ (M^+, *m/e* 516.2362) and significant fragmentation ions were observed at *m/e* 498.2215 ($M^+ - 18$), 456.2175 ($M^+ - 60$), 438.2057 ($M^+ - 60, -18$) and a diagnostic fragment at 163.0754 ($C_{10}H_{11}O_2$). Acetylation (acetic anhydride-pyridine) of amoorastatin (**2a**) led to a peracetate derivative (**2b**) corresponding to empirical formula $C_{34}H_{42}O_{12}$ (M^+, *m/e* 642): mp 225-228 °C; $[\alpha]^{22}_D$ −97.4° (*c* 0.99, chloroform). Comparison of the 250-MHz ^{1}H NMR spectra obtained from aphanastatin (**1**)[2] with those of amoorastatin (**2a**) and the peracetate derivative **2b** (Table I) revealed a substantial amount of structural information. By this means it was ascertained that the aphanastatin A-ring substitution pattern was modified and the hydroxyl group at

0002-7863/78/1500-7731$01.00/0

Table I. Proton Magnetic Resonance Spectra[a] of Amoorastatin (**2a**) and the Corresponding Peracetate (**2b**)

proton position	amoorastatin (**2a**)[b]	peracetate (**2b**)[c]
H-1	4.19 (d, J = 3.3)	5.11 (d, J = 3.0)
H-2	2.96 (t, J = 3.4)	2.76 (m)
	3.02 (t, J = 3.3)	2.60 (m)
H-3	5.55 (d, J = 3.4)	5.32 (d, J = 2.5)
H-7	3.72 (s)	4.82 (br s)
H-9	4.72 (s)	4.08 (s)
H-12	2.46 (s, 2 H)	2.39 (AB q, J = 18)
		2.54
H-15	3.72 (s)	3.58 (s)
H-17	2.74 (m)	2.68 (t, J = 11)
H-19	4.41 (AB q, J = 13.3)	4.40 (br s, 2 H)
	4.53	
H-21	7.11 (s)	7.11 (s)
H-22	6.12 (s)	6.10 (s)
H-23	7.36 (s)	7.24 (s)
H-28	4.98 (s)	5.80 (s)
Me	0.90	0.83
	1.10	1.12
	1.35	1.16
OAc	1.95	1.96
		2.02
		2.12
		2.16

[a] At 250 MHz, at 22 °C, with chemical shifts in parts per million and coupling constants in hertz. [b] In deuteriochloroform containing 20% pyridine-d_5. [c] In deuteriochloroform.

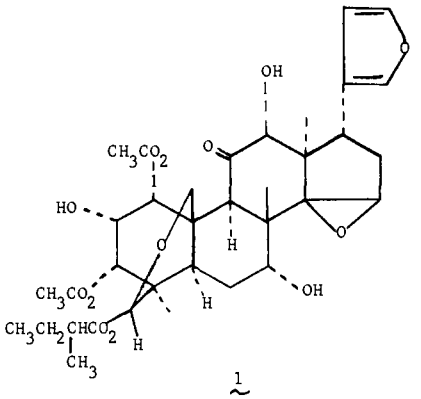

1

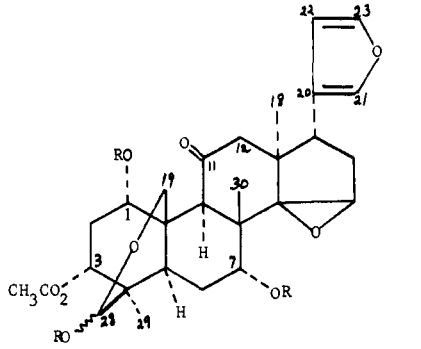

2a, R = H, amoorastatin
b, R = -C-CH$_3$ (O)

C-12 was missing. The monoacetylated 1,3-glycol system of the amoorastatin A ring was deduced by double resonance experiments. The chemical shifts for this system (δ_H, Table I, and δ_C, 70.8 (d) and 74.5 (d)) indicate the position of the acetate group to be at C-3.[6] The downfield shift obtained by acetylation of the C-28 hydroxyl group was characteristic of the hemiacetal unit and the C-15 proton at δ 3.72 clearly indicated[7] a 14,15 epoxide. The latter two assignments were further substantiated by inspecting the ^{13}C NMR (C-19 at 64.5 (t), C-28 at 96.2 and 95.9 (t), C-14 at 73.4 (s), and C-15 at 57.9 (d)).[6] The structure assigned, amoorastatin (**2a**), on the basis of these physical measurements was confirmed by a single-crystal X-ray analysis.

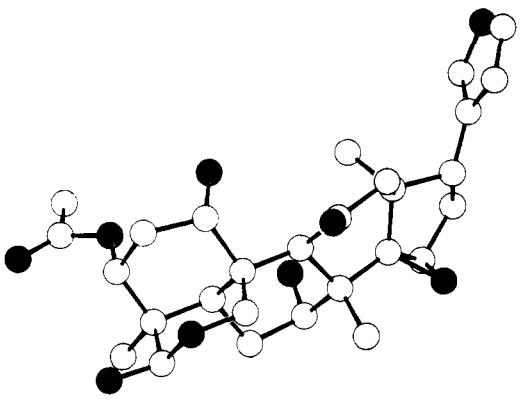

Figure 1. An ORTEP diagram of amoorastatin.

Amoorastatin (**2a** as the 28R epimer) crystallized with 1 mol of water (mp 170 °C) in the monoclinic form with space group $P2_1$; a = 7.780 (2), b = 12.818 (2), c = 13.003 (3) Å; β = 91.51 (3)°. The X-ray diffraction data were collected using a Philips PW 1100 diffractometer employing the ω-2θ scan technique with graphite monochromated Cu Kα radiation. The structural problem was solved using a Patterson search program[8] with the coordinates from the aphanastatin[2] ring system. A total of 1848 reflections was observed and a full-matrix least-squares refinement, with anisotropic temperature factors for the nonhydrogen atoms, resulted in an R factor of 0.052.

The three-dimensional view of amoorastatin (**2a**) shown in Figure 1 substantiates the substituent and configurational assignments as 1α-OH, 3α-OAc, 4α-CH$_3$, 5α-H, 7α-OH, 8β-CH$_3$, 9α-H, 11-oxo, 13α-CH$_3$, 14β,15β-epoxy, 17α-furan, and the hemiacetal ring incorporating carbon atoms C-19 and C-28. Both rings A and B are in the chair conformation and ring C is in a boat conformation. Ring D has assumed an envelope form with C-17 out of the mean plane passing through the other four atoms by 0.64 Å. The dihedral angles between H-7 and the two C-6 hydrogen atoms are −60 and +60°. Between H-15 and the two hydrogen atoms bonded to C-16 the dihedral angles are 48.6 and −73.5°.

Discovery of the structurally simpler amoorastatin (**2a**) with more pronounced cell growth inhibitory activity than aphanastatin (**1**) suggests that the 1α-acetoxy-, 2α- and 12α-dihydroxy-, and 28-α-methylbutyryl groups of aphanastatin are unnecessary and indeed may lessen inhibition of neoplastic (P388) cell growth.

Acknowledgments. We are pleased to thank M. C. Merienne (Laboratoire de RMN à Haut Champs, Orsay) for ^1H NMR measurements at 250 MHz, M. C. Marazano for high resolution mass measurements, Mme. C. Fontaine for the ^{13}C NMR spectra, and Linda M. Lange for assistance with biological experiments. The ASU CRI group gratefully acknowledges support of this investigation by Public Health Services Research Grant No. 16049-05 from the National Cancer Institute, the Fannie E. Rippel Foundation, Mrs. Mary Dell Pritzlaff, the Spencer T. and Ann W. Olin Foundation, Mr. John F. Schmidt, and the Phoenix Coca Cola Bottling Co.

References and Notes

(1) Antineoplastic Agents. 61. For part 60, refer to G. R. Pettit, M. T. Edgar, and T. S. Krupa, *J. Org. Chem.*, In press.
(2) J. Polonsky, Z. Varon, B. Arnoux, C. Pascard, G. R. Pettit, J. H. Schmidt, and

L. M. Lange, *J. Am. Chem. Soc.*, **100**, 2575 (1978).
(3) J. D. Connolly, K. H. Overton, and J. Polonsky, "Progress in Phytochemistry", Vol. II, L. Reinhold and Y. Liwschitz, Ed., Interscience, New York, 1970.
(4) The *Aphanamixis* genus has also been termed *Amoora*.
(5) G. R. Pettit, C. L. Herald, G. F. Judd, G. Bolliger, and P. S. Thayer, *J. Pharm. Sci.*, **64**, 2023 (1975); J. H. Schmidt and G. R. Pettit, *Experientia*, **34**, 659 (1978).
(6) M. Ochi, H. Kotsuki, K. Hirotsu, and M. Tokoroyama, *Tetrahedron Lett.*, 2877 (1976).
(7) J. W. Powell, *J. Chem. Soc. C*, 1794 (1966).
(8) B. P. Braun, J. Hornstra, and J. I. Leenhouts, *Philips Res. Rep.*, **24**, 85 (1969).

Judith Polonsky,* Zoia Varon
Bernadette Arnoux, Claudine Pascard
Institut de Chimie des Substances Naturelles
CNRS, 91190 Gif sur Yvette, France

George R. Pettit,* Jean M. Schmidt
Cancer Research Institute and Department of Chemistry
Arizona State University, Tempe, Arizona 85281

Received August 28, 1978

Remarks on Free-Energy Correlations of Rate Constants for Electron-Transfer Quenching of Electronically Excited States

Sir:

Following the pioneering work of Weller,[1] the electron-transfer quenching of electronically excited states has been actively investigated in the past decade.[2-8] In most of the systems studied, the quenching process was not accompanied by permanent chemical changes, indicating that the primary electron-transfer process is rapidly reverted in the dark. The elementary steps involved in a reversible electron-transfer quenching mechanism are shown in Scheme I.

The kinetics associated with such a scheme has been first worked out by Rhem and Weller[4,5] (RW) and their treatment has been thereafter followed by most workers in this field.[2,3,6-8] On the basis of steady-state considerations, the experimental bimolecular quenching constant, k_q, can be expressed as

$$k_q = \frac{k_{12}}{1 + (k_{21}/k_{23}) + (k_{21}k_{32}/k_{30}k_{23})} \quad (1)$$

The rate constants of the three electron-transfer steps in Scheme I, i.e., k_{23}, k_{32}, k_{30}, obey the general equation

$$k_{ij} = Z_{ij} \exp[-(\Delta G^{\ddagger}_{ij}/RT)] \quad (2)$$

where Z_{ij} is the frequency factor and $\Delta G^{\ddagger}_{ij}$ is the activation free energy of the process. If eq 2 is substituted into eq 1 for all three electron-transfer steps, the following equation

$$k_q = \frac{k_{12}}{1 + \dfrac{k_{21}}{Z_{23}\exp\left(-\dfrac{\Delta G^{\ddagger}_{23}}{RT}\right)} + \dfrac{k_{21}}{Z_{30}\exp\left(-\dfrac{\Delta G^{\ddagger}_{30}}{RT}\right)}\exp\left(\dfrac{\Delta G_{23}}{RT}\right)} \quad (3)$$

is obtained, where ΔG_{23} is the overall free-energy change associated with the forward electron-transfer process. In their classical work,[4,5] RW assume that k_{30} can be taken as a common frequency factor, Z, for all three electron-transfer processes because "since the free energy gained in . . . k_{30} . . . is exceedingly large, $\Delta G^{\ddagger}_{30}$ can be assumed to be close to zero". This simplifying assumption leads to the following expression for the bimolecular quenching constant:

$$k_q = \frac{k_{12}}{1 + (k_{21}/Z)[\exp(\Delta G^{\ddagger}_{23}/RT) + \exp(\Delta G_{23}/RT)]} \quad (4)$$

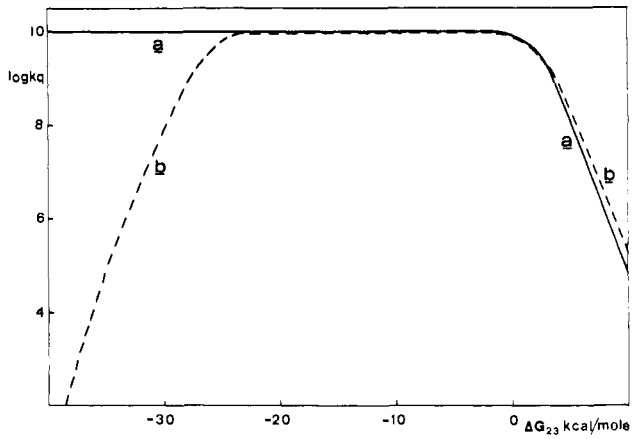

Figure 1. Free-energy correlation of rate constants for electron-transfer quenching calculated[10] from eq 4 plus eq 6 (curve a) or eq 5 (curve b).

Scheme I

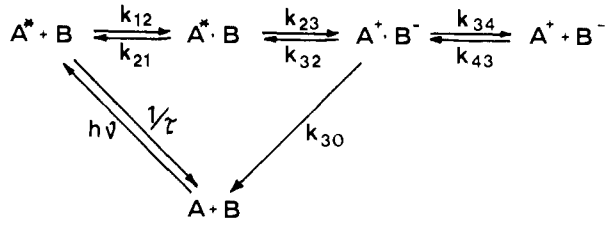

This expression can be used to calculate the dependence of the bimolecular quenching constant on the overall free-energy change, provided that a functional relationship between $\Delta G^{\ddagger}_{23}$ and ΔG_{23} is assumed. Two options are presently available in this regard. The first one is the classical relationship from the Marcus theory[9] of outer-sphere electron transfer reactions:

$$\Delta G^{\ddagger}_{ij} = \Delta G^{\ddagger}_{ij}(0)\{1 + [\Delta G_{ij}/4\Delta G^{\ddagger}_{ij}(0)]\}^2 \quad (5)$$

The second one is an empirical relationship proposed by RW:[4,5]

$$\Delta G^{\ddagger}_{ij} = \{[(\Delta G_{ij}/2)]^2 + [\Delta G^{\ddagger}_{ij}(0)]^2\}^{1/2} + (\Delta G_{ij}/2) \quad (6)$$

In eq 5 and 6, $\Delta G^{\ddagger}_{ij}(0)$ is the activation free energy the reaction should have if no overall free energy change occurred, a quantity often called the "intrinsic barrier" to the electron-transfer process.

The dependence of the bimolecular quenching constant on the overall free-energy change predicted by eq 4 after substitution with eq 5 or eq 6 is shown in Figure 1. Curve b is calculated using the Marcus expression (eq 5), while curve a is calculated using the RW one (eq 6).[10] Both plots have an almost identical Arrhenius-type portion in the endoergonic region and a plateau in the slightly exoergonic region, but a sharp difference between the two curves shows up in the highly exoergonic region. In this region, according to RW the quenching constants remain on the plateau, whereas according to Marcus they should exhibit a sharp drop, usually called "inverted" behavior. The highly exoergonic region has only been specifically investigated in a limited number of studies.[2,3,6-9] However, the available experimental results clearly show that the RW relationship (eq 6) is obeyed, while no clear evidence for inverted behavior has so far been reported.[11]

In this communication, we would like to point out a particular feature of this kinetic system which seems to have been largely overlooked in the past. It should be realized that the ability of the Marcus (eq 5) or RW (eq 6) relationships to interpret the experimental results cannot be tested by introducing these equations into eq 4, since this equation originates from an assumption (i.e., $k_{30} \approx Z$) which already implies an anti-Marcus behavior for the back-electron-transfer step. Rather,

0002-7863/78/1500-7733$01.00/0